Mon. Not. R. Astron. Soc. **289,** 801–812 (1997)

The supercluster–void network – II. An oscillating cluster correlation function

J. Einasto,[1] M. Einasto,[1] P. Frisch,[2] S. Gottlöber,[3] V. Müller,[3] V. Saar,[1] A. A. Starobinsky,[4] E. Tago,[1] D. Tucker[3,5] and H. Andernach[6,7]

[1]*Tartu Observatory, EE-2444 Tõravere, Estonia*
[2]*Göttingen University Observatory, Geismarlandstr. 11, D-37083 Göttingen, Germany*
[3]*Astrophysical Institute Potsdam, An der Sternwarte 16, D-14482 Potsdam, Germany*
[4]*Landau Institute Theoretical Physics, Moscow 117334, Russia*
[5]*Fermilab, MS 127, PO Box 500, Batavia, IL 60510, USA*
[6]*INSA, ESA IUE Observatory, E-28080 Madrid, Spain*
[7]*Depto de Astronomía, Univ. Guanajuato, Guanajuato, Mexico*

Accepted 1997 March 23. Received 1997 February 26; in original form 1996 December 2

ABSTRACT

We use rich clusters of galaxies in the Northern and Southern Galactic hemispheres up to a redshift $z = 0.12$ to determine the cluster correlation function for a separation interval $\approx 650\,h^{-1}$ Mpc (h is the Hubble constant in units of 100 km s^{-1}Mpc^{-1}). We show that superclusters of galaxies and voids between them form a moderately regular network. As a result the correlation function determined for clusters located in rich superclusters oscillates: it has a series of regularly spaced secondary maxima and minima. The scale of the supercluster–void network, determined from the period of oscillations, is $P = 115 \pm 15\ h^{-1}$ Mpc. Five periods are observed. The correlation function found for clusters in poor and medium-rich superclusters is zero on large scales. The correlation functions calculated separately for the Northern and Southern Galactic hemispheres are similar; only the amplitude of oscillations for clusters in the Southern hemisphere is larger by a factor of about 1.5.

We investigate the influence of possible errors in the correlation function. The amplitude of oscillations for clusters in very rich superclusters is about 3 times larger than the estimated error. We argue that the oscillations in the correlation function are due neither to the double-cone shape of the observed volume of space, nor to the inaccuracy in the selection function.

We compare the observed cluster correlation function with similar functions derived for popular models of structure formation, as well as for simple geometrical models of cluster distribution. We find that the production of the observed cluster correlation function in any model with a smooth transition of the power spectrum from a Harrison–Zeldovich regime with positive spectral index at long wavelengths to a negative spectral index at short wavelengths is highly unlikely. The power spectrum must have an extra peak located at a wavelength equal to the period of oscillations of the correlation function. The relative amplitude of the peak over the smooth spectrum is probably of the order of a factor of at least 1.25.

These quantitative tests show that high-density regions in the Universe marked by rich clusters of galaxies are distributed more regularly than expected. Thus our present understanding of structure formation needs revision.

Key words: galaxies: clusters: general – cosmology: observations – cosmology: theory – large-scale structure of Universe.

1 INTRODUCTION

A fundamental property of the distribution of galaxies is clustering, manifested by the presence of groups and clusters of galaxies and quantitatively measured by the correlation function. Owing to clustering, the correlation function of galaxies has a large positive value at small separations. At a separation of $\sim 30\ h^{-1}$ Mpc the correlation function approaches (or crosses) zero and remains small on larger scales. A correlation function of zero has been interpreted as an indication of a random distribution of galaxies.

This picture – clustering on small scales and a random scale-free distribution on larger scales – formed the classical paradigm of the large-scale distribution of galaxies and clusters of galaxies.

The discovery of superclusters consisting of clusters and filaments of galaxies and huge voids between them has changed this classical paradigm. According to available data, superclusters reside in chains and walls, separated by voids of diameters of about $100\,h^{-1}$ Mpc, and form a rather regular network (Einasto et al. 1994; Einasto et al. 1997c, hereafter Paper I). This raises a question about the existence of some regularity in the distribution of superclusters of galaxies, and, if so, about the presence of a related scale in the Universe.

The first clear demonstration of the possible presence of a regularity in the distribution of galaxies on very large scales came from a deep pencil-beam survey of galaxies by Broadhurst et al. (1990). This survey covers small areas near the North and South Galactic poles and has a depth of about 700 h^{-1} Mpc in both directions. The galaxy density shows periodic peaks separated by $\sim$128 h^{-1} Mpc. In total over 10 peaks have been observed. Bahcall (1991) explained high-density regions in the distribution of galaxies by the presence of superclusters.

There has been much discussion regarding the implication of this result. Kaiser & Peacock (1991) have argued that a peak in the one-dimensional spectrum can arise without any large-scale feature in the three-dimensional distribution of galaxies. Dekel et al. (1992) investigated the problem and showed that this periodicity is barely compatible with Gaussian fluctuations in the framework of cold dark matter (CDM)-type scenarios of structure formation. Thus the initial reaction to the observation of Broadhurst et al. was that there is no need to change the classical paradigm on the distribution of matter on large scales.

However, other independent data on the possible presence of some regularity in the distribution of matter on large scales in the Universe have accumulated. In the 1970s Shvarzman and Kopylov initiated a programme to study the large-scale distribution of matter. They used Abell (1958) clusters of galaxies of richness $R \geq 2$, and rich, compact clusters from the list of Zwicky et al. (1961–68); redshifts were determined for clusters up to $z \approx 0.3$ in a region around the North Galactic pole. This survey indicated the presence of a secondary peak in the correlation function at $\approx$125 h^{-1} Mpc (Kopylov et al. 1984, 1988). Later the survey was extended to the Southern Galactic hemisphere, and a peak in the correlation function on the same scale was found (Fetisova et al. 1993). Mo et al. (1992a,b) and Einasto & Gramann (1993) used a different method to analyse the cluster correlation function, and the presence of a feature at $\sim 130\,h^{-1}$ Mpc was confirmed. A similar scale was found in the distribution of clusters using other methods like the void and pencil-beam analysis (Einasto et al. 1994; Paper I).

Landy et al. (1996) derived the 2D power spectrum of the Las Campanas Redshift Survey and found a peak at a wavelength of 100 h^{-1} Mpc. The peak is due to numerous density enhancements located at this characteristic mutual separation. The same redshift survey was also analysed by Tucker et al. (1995, 1997) and Doroshkevich et al. (1996) who also found characteristic features on similar scales. An $\sim 100\,h^{-1}$ Mpc scale has also been seen in the distribution of QSO absorption-line systems (Quashnock, Vanden Berk & York 1996).

During the past few years the number of redshifts determined for rich clusters of galaxies has rapidly increased. This makes a new analysis of cluster data worthwhile, as the Abell–ACO cluster sample (see next section) is the deepest almost full-sky survey available at present. In this paper we study the correlation function for clusters of galaxies using a recent compilation of available data on clusters of galaxies by Andernach, Tago & Stengler-Larrea (1995 and in preparation). Our study follows approaches by Bahcall & Soneira (1983) and more recently by Peacock & West (1992) and Einasto et al. (1993). However, in contrast to all previous studies we concentrate here on large scales, i.e. well beyond 100 h^{-1} Mpc. To do this we consider the whole data set of clusters now available for both the Northern and Southern Galactic hemispheres as a single sample of depth $\approx$700 h^{-1} Mpc. The same data set has been used in Paper I to derive a catalogue of superclusters of galaxies and to study the spatial distribution of clusters, by Jaaniste et al. (in preparation) to investigate the orientation and shape of superclusters of galaxies, and by Saar et al. (1995) to determine the correlation function with a novel method. Problems of methodology connected with the determination and interpretation of the correlation function on large scales are discussed separately by Einasto et al. (1997b, hereafter Paper III). The power spectrum for our cluster sample was found and discussed by Einasto et al. (1997a, hereafter E97).

The paper is structured as follows. In Section 2 we describe the observational data used and the selection functions of the data. Section 3 is devoted to the analysis of the correlation function of clusters of galaxies on large scales. We determine the correlation function for the whole sample as well as for subsamples of clusters in the Northern and Southern Galactic hemispheres, and for cluster populations located in rich and poor superclusters. In Section 4 we discuss the influence of the smoothing length, inaccuracy of the selection function, and other factors on our results. In Section 5 we compare our results with simulations using simple geometrical models and results of N-body calculations for the CDM model and a double-power-law model. In Section 6 we derive the possible cluster power spectrum from models. A summary of the main results is given in Section 7.

We use a Hubble constant of $H_0 = 100\,h\,\mathrm{km\,s^{-1}\,Mpc^{-1}}$.

2 DATA

The Abell–ACO catalogue of clusters of galaxies (Abell 1958; Abell, Corwin & Olowin 1989) is presently the largest available source of the large-scale distribution of matter in the Universe covering the whole sky outside the Milky Way zone of avoidance. We use for the present study a recent compilation of measured redshifts for these clusters by Andernach et al. (in preparation). This compilation gives redshifts for a total of about 2000 Abell–ACO clusters (including supplementary, or S-clusters). We used the 1995 version of the compilation, omitted all S-clusters and used only clusters with measured redshifts up to $z = 0.12$. To this sample we added all clusters with photometric redshift estimates $z_{\mathrm{est}} \leq 0.12$. Our full sample contains 1304 Abell–ACO clusters of galaxies, 869 of which have measured redshifts.

We have included clusters of richness class 0 in our study. About half of all clusters in the nearby region studied are of this richness class, and the number of objects is crucial in the present work. Abell clusters of richness class 0 are X-ray emitters and hosts of cD galaxies with extended haloes as often as are clusters of higher richness. Both facts suggest that these clusters are physical objects which can be used to trace the large-scale structure. Possible projection effects discussed by Sutherland (1988), Dekel et al. (1989) and others are not crucial for the present study, as we are mostly interested in the distribution of clusters on large scales. A small excess of cluster pairs at small separations noted by Sutherland and Dekel et al. can be considered as an additional selection effect.

This sample was used in Paper I to derive a new catalogue of superclusters and to study their spatial distribution. In the present paper we use both the cluster sample and the supercluster catalogue. The use of the supercluster catalogue gives us the possibility of analysing the distribution of clusters in different environments. Superclusters were determined using a 'friends-of-friends' technique with neighbourhood radius $24\,h^{-1}$ Mpc. This radius was chosen on the basis of the multiplicity function which shows that individual superclusters start to become evident at a neighbourhood radius of about 16 h^{-1} Mpc; at radii larger than 30 h^{-1} Mpc, superclusters begin to join into huge agglomerates with dimensions exceeding the characteristic scale of the supercluster–void network. Thus the neighbourhood radius must lie within these boundaries. The influence of this radius on our results for the correlation function will be studied below (Section 4.3).

In Paper I superclusters were divided into richness classes according to their multiplicity (the number of member clusters in superclusters). It was also shown that the overall distribution of superclusters of different richness is rather similar to each other: superclusters are located in chains that form a fairly regular network. The mean diameter of voids between superclusters is ~ 100 h^{-1} Mpc. The skeleton of the supercluster–void network is formed by very rich superclusters. Poor and medium-rich superclusters as well as isolated clusters are scattered around them, leaving void interiors empty of rich clusters. The distribution of superclusters in void walls depends on the supercluster richness: the mean separation between poor and medium-rich superclusters is small and has a smooth distribution, whereas the separation between very rich superclusters is much larger and its distribution is peaked: over 75 per cent of very rich superclusters are located at separations of 110–150 h^{-1} Mpc on opposite sides of voids.

This finding motivated us to study the correlation function of clusters of galaxies located in superclusters of different richness. As in Paper I we divide cluster samples into populations using the supercluster richness as the parameter that determines *the mean density of the large-scale environment* of clusters (see Frisch et al. 1995). In contrast to Paper I, we divide superclusters into only two richness classes with variable richness threshold. We shall use the following nomenclature for cluster samples. The first three capital letters ACO denote clusters from the Abell–ACO catalogue (excluding S-clusters); the following capital letter indicates whether we use the sample of all clusters (A) or the sample of clusters with measured redshifts (R); the following capital letter denotes cluster samples in high- or low-density environments (respectively H or L); the last number indicates the limiting multiplicity $N_{\rm cl}$ of superclusters used to divide the sample into high- and low-density populations. Clusters belonging to superclusters with *at least* $N_{\rm cl}$ members are attributed to the high-density population, and isolated clusters as well as clusters in superclusters with *fewer* than $N_{\rm cl}$ members to the low-density population.

To calculate the correlation function of clusters of galaxies we generate Poisson samples of test particles with the same shape and selection function as the real samples. The selection effects depend on Galactic absorption, on the difficulty of finding lower richness clusters at large distances, on the decrease in the fraction of clusters with measured redshifts with distance, on the differences in the mean density of clusters in the Abell and ACO catalogues, etc.

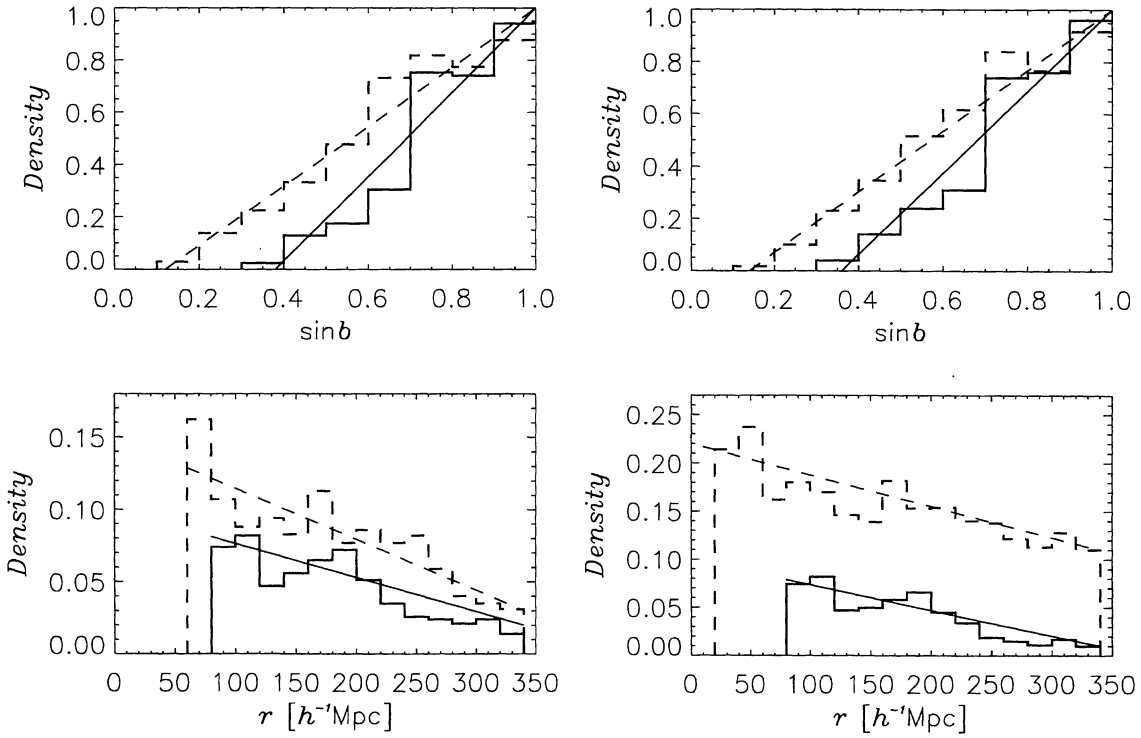

Figure 1. Selection functions for clusters of galaxies. The volume density of clusters is shown as function of the sine of Galactic latitude b (upper panels) and as function of distance r from the observer (lower panels). In the upper panels the density is given in units of the density near the Galactic pole (i.e. $\sin b = 1$); in the lower panels it is given in arbitrary units. In the left-hand panels only clusters with measured redshifts were used; in the right-hand panels we used all clusters. Dashed lines are for clusters located in low-density environments (isolated clusters and clusters in superclusters with fewer than eight members); solid lines are for high-density regions (clusters in superclusters with at least eight members). Dashed and solid straight lines represent linear approximations of the selection function.

Table 1. Selection function parameters.

Sample	s_0	d_{0N}	d_{1N}	d_{0S}	d_{1S}
ACO.R.H8	0.38	1.00	0.80	1.00	0.80
ACO.R.L8	0.12	1.00	0.80	1.00	0.80
ACO.A.H8	0.36	1.00	0.50	1.00	0.50
ACO.A.L8	0.14	0.78	0.36	1.00	0.52

Poisson samples must be generated with all these effects taken into account. We have calculated the selection function as a function of two variables, the Galactic latitude b, and the distance from the observer r, separately for the Northern and Southern Galactic hemispheres. We determined selection functions for clusters populating rich and poor superclusters, using a threshold richness of $N_{cl} = 8$. The influence of the choice of the threshold richness N_{cl} will be discussed in the next section.

In Fig. 1 we show the results of the determination of the selection function for clusters of galaxies with measured redshifts. The number of clusters versus the Galactic latitude was determined as a function of $\sin b$. Differences between the two hemispheres are small, thus in Fig. 1 we present the mean of both hemispheres. Data are normalized to unit density at $\sin b = 1$. We see an almost linear decrease of the number density of clusters with $\sin b$. This linear regression, $D(b) = (\sin b - \sin b_0)/(1 - \sin b_0)$, is given by the value $s_0 = \sin b_0$ where the density of cluster reaches 0, and it was used to calculate Poisson samples for the correlation function.

To determine the distance dependence of the selection function, the spatial density of clusters of galaxies was calculated in concentric spherical shells of thickness 20 h^{-1} Mpc, for each hemisphere separately. Fluctuations are rather large, thus for this sample of clusters the mean regression was derived for both hemispheres. The spatial density can be represented by a linear law: $D(r) = d_0 - d_1(r/r_1)$, where d_0 and d_1 are constants, and r_1 is the outer radius of the sample. Values of the selection function parameters d_0 and d_1, found for various subsamples of clusters, are given in Table 1.

A similar analysis of the selection function was made for the sample of all 1304 clusters. Here, too, the sample was divided into high- and low-density populations using the same threshold $N_{cl} = 8$. Table 1 shows that parameters of the distance dependence in the Northern and Southern hemispheres (denoted with subscripts N and S, respectively) are identical in most cases. Only the cluster sample of all clusters in low-density regions is large enough to determine parameters of the distance dependence separately for both hemispheres. Here d_{0N} is smaller than d_{0S}, which reflects the fact that the number density of the Northern cluster sample is lower than that of the Southern one. Parameters for the selection effect in Galactic latitude are similar for the sample of all clusters and for that of clusters with measured redshifts.

3 THE CLUSTER CORRELATION FUNCTION

3.1 Deep cluster samples

In this section we discuss the correlation function of Abell–ACO clusters of galaxies in various environments. As noted above, clusters in high-density environments (rich superclusters) form a fairly regular three-dimensional network, whereas clusters in low-density environments (isolated clusters and clusters in poor and medium-rich superclusters, or simply poor superclusters) are located in their vicinity more irregularly (Paper I). To determine which limiting richness N_{cl} divides clusters naturally into high- and low-density environments, we calculated the correlation functions for both populations using limiting richnesses between $N_{cl} = 1$ and 8. For $N_{cl} = 1$ by definition there are no clusters in the low-density population (since the low-density population consists of clusters in superclusters of multiplicity less than N_{cl}). Results for $N_{cl} = 1, 4$ and 8 are shown in Figs 2 and 3 for clusters with measured redshifts.

These figures show that the correlation function of clusters in rich superclusters has a number of quasi-regularly spaced secondary maxima and minima (in addition to the main maximum at small separation). This phenomenon is the main finding of the present paper and we shall refer to it as the *oscillation* of the correlation function.

In contrast to the correlation function of clusters in rich superclusters, the correlation function of clusters in poor superclusters approaches zero smoothly after the initial maximum. The nearest neighbour test and void analysis show (Paper I) that clusters in poor superclusters are located more irregularly in void walls between rich superclusters, and thus secondary peaks of the correlation function owing to individual poor superclusters cancel each other out.

Parameters of the oscillations of the correlation function for clusters in rich superclusters are given in Table 2: N is the number of clusters in the sample; r_{min} is the location of the first secondary minimum of the correlation function; r_{max} is the location of the first secondary maximum; A_{max} is the amplitude, which is defined as half of the difference of the values of the correlation function between the first secondary maximum and minimum; σ_ξ is the mean 1σ error of the correlation function, which determines the width of the error corridor; Δ_{21} and Δ_{32} are distances between secondary maxima indicated by the respective indices; and Δ_{mean} is the mean separation of the secondary maxima, and of the secondary minima. Positions of the maxima and minima and differences between them are given in h^{-1} Mpc. The mean error was calculated from equation (16) of Paper III. Essentially the error is determined by the cosmic variance (i.e. the variation of the correlation function in different volumes of space):

$$\sigma_{\xi c} = \frac{b}{\sqrt{N}}, \tag{1}$$

where b is a parameter introduced in Paper III to describe the dependence of the error on the character of the large-scale distribution of clusters of galaxies. It must be determined from mock samples. We have done this (for details see Paper III) and found that $b \approx 1.5$ (see also the discussion in section 4). As we see from the above equation, the width of the error corridor for the cosmic variance is constant.

We see from Table 2 that the amplitude of oscillations increases with the increase of the minimum supercluster richness N_{cl}. This leads us to the conclusions that, for low values of N_{cl}, we actually have a mixture of populations in the high-density population, and that the proper division of populations occurs at the highest minimum richness, $N_{cl} = 8$. To check this result we have calculated the correlation function separately for clusters located in superclusters of medium-richness, from $N_{cl} = 4$ to 7. The correlation function of this subpopulation shows only marginal signs of oscillations. Thus we can accept $N_{cl} = 8$ as the limiting richness to select the regularly distributed population of clusters in rich superclusters. This analysis confirms results found in Papers I and III: a smooth distribution in void walls leads to a non-oscillating correlation function in the case of clusters in poor superclusters;

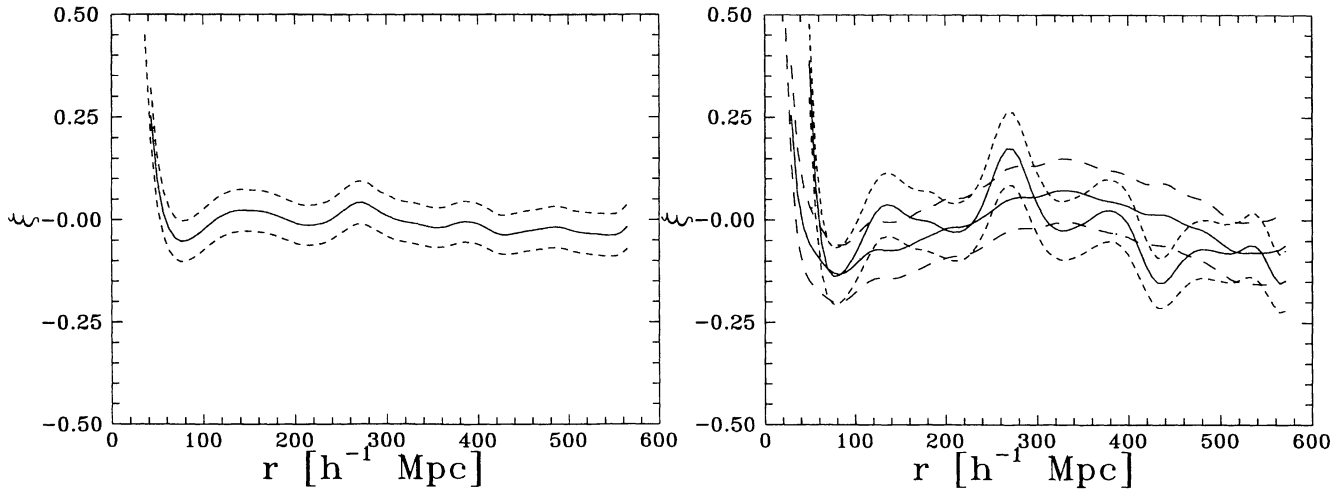

Figure 2. The correlation function of clusters of galaxies with measured redshifts. The left-hand panel is for the sample of all clusters (ACO.R.H1). In the right-hand panel, data on high- and low-density populations are given separately. Solid lines show the correlation function; the error corridor for high- (ACO.R.H4) and low-density (ACO.R.L4) cluster populations is marked with short and long-dashed lines, respectively. The overall curved shape of the correlation function is due to cosmic variance (compare with fig. 7 of Paper III).

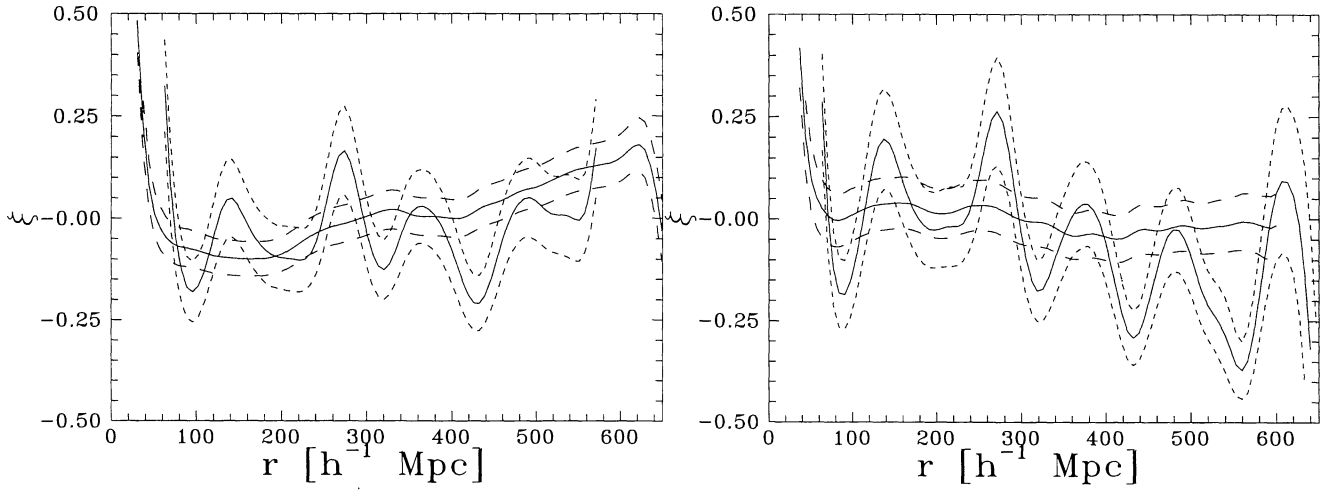

Figure 3. The correlation function for all clusters (samples ACO.A.H8 and ACO.A.L8 in the left-hand panel), and for clusters with measured redshifts (samples ACO.R.H8 and ACO.R.L8 in the right-hand panel). Solid, long-dashed and short-dashed lines have the same meaning as in Fig. 2.

oscillations occur only in the case of rich superclusters located in a quasi-regular rectangular lattice.

In Table 2 we give parameters of the oscillating correlation function for the cluster population with measured redshifts. The sample of all clusters was also divided into high- and low-density populations, and parameters of the correlation function were determined. Results for samples with measured redshifts and for all clusters are given in Fig. 3. In this case we see that, on large scales, clusters in rich superclusters have an oscillating correlation function and clusters in poor superclusters have a zero correlation. Parameters of the oscillations of clusters in rich superclusters have values very close to those for the sample of clusters with measured redshifts; only the amplitude of oscillations is smaller by a factor of about 1.5. A smaller amplitude for the sample of all clusters is likely, owing to the larger observational errors in the photometric redshifts, which smooth out features slightly in the correlation function.

Now we compare the errors in the correlation function for subsamples with various limiting richnesses $N_{\rm cl}$. We see that the amplitude of oscillations for the sample ACO.R.H8 is approximately three times larger than the error: i.e. we are able to establish the presence of oscillations at the 3σ level. For the sample of clusters of all richness classes taken together (ACO.R.H1) the error is approximately equal to the amplitude of oscillations. This shows that the division of clusters into high- and low-density populations is crucial *to demonstrate the presence of oscillations*. (We note, however, that the power spectrum of the cluster population in rich superclusters is almost identical in shape to the spectrum of the whole cluster population.)

3.2 Cluster samples in the Northern and Southern hemispheres

Now we determine the cluster correlation function separately for the Northern and Southern Galactic hemispheres. To increase the number of clusters we use the sample of all clusters, and divide this sample again into rich and poor superclusters using the limiting

Table 2. Parameters of the correlation function for various cluster samples.

Sample	N	r_{min}	r_{max}	A_{max}	σ_ξ	Δ_{21}	Δ_{32}	Δ_{mean}
ACO.R.H1	869	78	144	0.056	0.051	126	116	122
ACO.R.H2	624	79	131	0.056	0.060	137	117	122
ACO.R.H4	433	78	136	0.134	0.072	134	108	123
ACO.R.H6	331	83	140	0.200	0.082	132	108	120
ACO.R.H8	261	88	138	0.279	0.093	133	104	116
$ACO.A.H8_N$	152	94	133	0.069	0.130	132	103	118
$ACO.A.H8_S$	167	97	143	0.275	0.124	140	105	118

richness $N_{cl} = 8$. Fig. 4 shows the correlation function of clusters located in rich superclusters separately for both Galactic hemispheres. We see that there are some differences between the correlation functions.

The oscillatory behaviour is very clear in both cases, and the periods of oscillation are identical (see Table 2). The basic difference lies in the amplitude, which is smaller for the Northern hemisphere. This suggests that the supercluster–void network is less regular in the Northern hemisphere. It is interesting to note that Landy et al. (1996) have determined the power spectrum of galaxies in the deep Las Campanas Redshift Survey separately for the Northern and Southern Galactic hemispheres. The Southern samples have a strong peak at a wavelength $\approx 100\,h^{-1}$ Mpc, whereas in Northern samples this feature is much weaker. The similarity of these independent measures of the regularity of the structure suggests, first of all, that both methods (the correlation and spectral analyses) work and that they measure the large-scale regularity of the structure. Secondly, these results indicate that there are small but definite differences in the large-scale distribution of high-density regions in the nearby Universe. In other words, Northern and Southern samples, taken separately, do not form fair samples of the Universe.

3.3 Mean parameters of oscillations

The grid size or step of the supercluster–void network can be determined from data given in Table 2 using relations between the step and parameters given in Paper III. All scaling parameters depend on the period P which is equal to the step of the supercluster–void network (see section 4.4 of Paper III). The most accurate value of the period comes from the relation $P = \Delta_{mean}/1.01$; here Δ_{mean} is the mean separation between maxima and between minima. We obtain

$$P = 115 \pm 15\,h^{-1}\mathrm{Mpc}. \quad (2)$$

The variance of the mean period is given mainly by the error of the positions of the last maximum and minimum. The error in the location of the outermost extrema is $25\,h^{-1}$ Mpc, which contributes an error of $5\,h^{-1}$ Mpc in P. The actual error is larger, as we must take into account also possible cosmic scatter of the step in different volumes. Comparison of different subsamples yields the error estimate given in (2). We note that the value of the period of oscillations is very close to the mean separation between rich superclusters located on opposite sides of voids. The latter separation was found to be $120\,h^{-1}$ Mpc in Paper I.

The amplitude of oscillations is given by the amplitude of the first secondary maximum for clusters with measured redshifts located in rich superclusters:

$$A = 0.28 \pm 0.05. \quad (3)$$

The error of the amplitude is estimated on the basis of the scatter of estimates of the amplitude for different subsamples and of the Poisson error of the data.

3.4 The parameters of the correlation function

Here we determine the numerical relations between various parameters of the correlation function. As demonstrated in Paper III, the separation of the first secondary maximum of the correlation function from zero is always larger than the period of oscillations, and the difference between the second and first secondary maxima is always larger than the difference between the third and second secondary maxima.

Using the observed correlation function parameters in Table 2 we have found the following relations: $f_1 = r_{max}/P = 1.20$; $f_{21} = \Delta_{21}/P = 1.16$; and $f_{32} = \Delta_{32}/P = 0.84$; where Δ_{21} and Δ_{32} are mean separations of respective maxima of the correlation function. A comparison of numerical values for these parameters

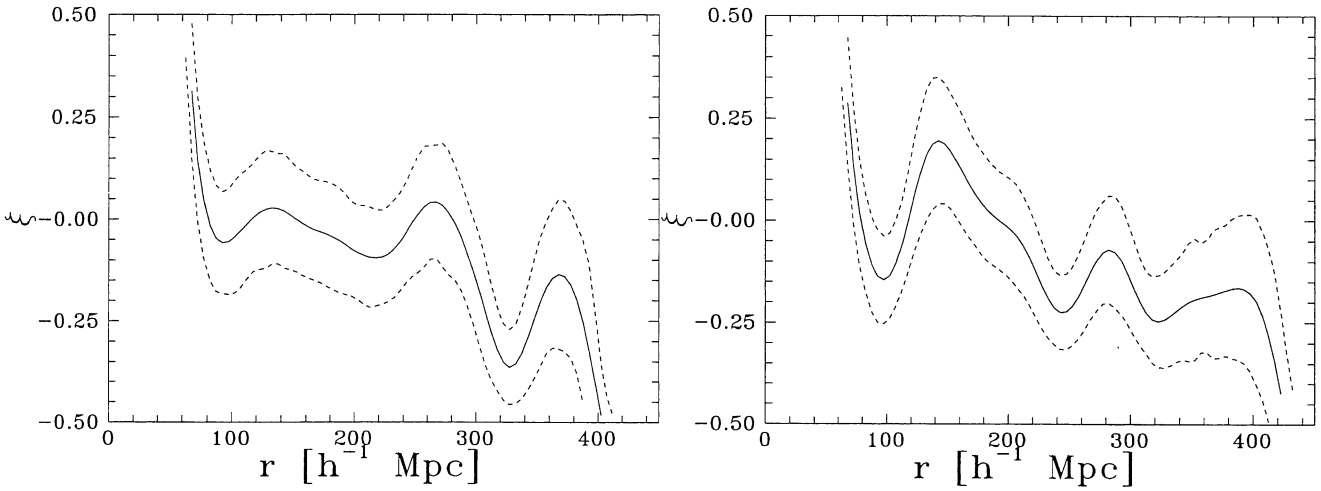

Figure 4. The correlation function calculated separately for the Northern (left-hand panel) and Southern (right-hand panel) Galactic hemispheres for all clusters located in rich superclusters. Error corridors are also given.

with respective values found for model samples in Paper III shows a rather close agreement. This agreement is an additional argument indicating the reality of our results.

3.5 The correlation length

In this paper the major emphasis is on the study of the correlation function of clusters of galaxies on large scales. Our data contain information also on the correlation function on small scales, and in this section we discuss our results for the determination of the correlation length. This parameter is defined as the value of the separation $r = r_0$ at which the correlation function $\xi(r_0) = 1$. This parameter depends critically on the characteristic size of superclusters.

We determined the correlation length using non-smoothed correlation functions, since smoothing increases it. As for other parameters, the correlation length was found separately for cluster samples in rich and poor superclusters. The results are interesting: for clusters in rich superclusters the correlation length is

$$r_0 = 46 \pm 5\, h^{-1}\mathrm{Mpc}, \tag{4}$$

and for clusters in poor superclusters it is

$$r_0 = 17 \pm 3\, h^{-1}\mathrm{Mpc}. \tag{5}$$

The errors are estimated on the basis of the scatter from samples for various minimum multiplicity values. Differences in the correlation function at small scales are also seen in Figs 2 and 3, although the smoothing makes the correlation length appear larger.

These differences are expected when we take into account the geometric meaning of the correlation length – it is close to the mean minor diameter of systems of clusters. Poor superclusters are small, but rich ones have much larger diameters (Jaaniste et al, in preparation). Similar differences are found also for clusters in rich and poor superclusters in models (Paper III). These calculations show that there exists no unique correlation length for clusters; it is in fact a function of cluster environment (the size of superclusters).

4 TESTING THE REALITY OF OSCILLATIONS

The presence of oscillations in the cluster correlation function was first established by one of us (VS) in 1994 December and presented in a preprint by Saar et al. (1995). Since then we have discussed this result at several conferences and seminars. During these discussions a number of questions were raised. Perhaps the local minima and maxima of the correlation function are just a random noise or due to selection effects, supercluster definition, smoothing, or some other disturbing effect? And if oscillations are real, can they be reproduced in the framework of conventional CDM cosmogony with Gaussian initial fluctuations, or do they demand a radical change of our paradigms on the formation of structure in the Universe? To answer these questions we have performed a number of tests. In this section we discuss the reality of oscillations.

4.1 Errors in the correlation function

The most serious question is related to errors in the correlation function. Often the errors in the correlation function are calculated from Poisson statistics. Mo, Jing, & Börner (1992c) have shown that the cosmic variance is much larger than the Poisson noise, and our results have confirmed this. Einasto & Gramann (1993) determined the error corridor by a bootstrap procedure. This method is also not very accurate since it cannot handle real variance of samples in different volumes of space. The only way to get an idea of the possible effect of this cosmic variance is to study various models of the cluster distribution.

Results of this study are presented in detail in Paper III. It is shown that the error corridor of the correlation function due to cosmic variance depends on the size of the sample (the number of particles N) and the nature of the distribution of particles, and can be parametrized by equation (1) presented above. The parameter b of this equation has a value of $b \approx 1.5$ in models that have a large-scale distribution of clusters similar to the observed distribution. In our calculations we have used this value of the error parameter. The amplitude of oscillations of the correlation function for the subsample of clusters in rich superclusters, ACO.R.H8, is about 3 times larger than the error; thus cosmic errors do not play an important role. If we use the sample of all clusters with redshifts (ACO.R.H1) then the amplitude of the correlation function is approximately equal to the cosmic variance (cf. Fig. 2). Thus it is essential to divide the cluster sample into two populations with different properties of the spatial distribution to establish the oscillatory behaviour of the cluster correlation function.

4.2 Sample shape

Since the sample volume has the form of a double cone and is restricted to a limiting distance, we will now check whether the curious shape of the sample can artificially generate oscillations in the correlation function.

The strongest evidence against such an effect comes from the comparison of samples in rich and poor superclusters (cf. Figs 2 and 3). Both samples occupy an identical double-cone-shaped volume. The only difference lies in the spatial distribution of clusters *within* the double-conical volume. It is very difficult to assume a selective influence of the sample volume shape, so that in the case of clusters in rich superclusters the shape generates oscillations in the correlation function, and in the case of clusters in poor superclusters it produces a smooth correlation function near zero. The difference must be intrinsic.

To investigate this problem we have studied in Paper III the influence of the sample shape on the correlation function. Results show that the double-conical sample has about a factor of 4 fewer particles than the whole cubical sample, and thus cosmic variance is larger, but the value of the error parameter b is almost the same as for the whole cubical sample. In the cases in which structural elements (clusters in high-density regions) led to an oscillatory behaviour of the correlation function, these were present in sufficient quantity also when restricting the sample volume to a double cone. If the size of the conical sample is very small, then characteristic elements that determine the oscillating properties of the correlation function are not present in sufficient quantities and the correlation function becomes irregular.

4.3 Supercluster selection

The supercluster catalogue used in this study was compiled in Paper I using a neighbourhood radius of $24\, h^{-1}$ Mpc. Is this radius crucial for the oscillatory behaviour of the correlation function?

The dependence of the supercluster catalogue on the neighbourhood radius was investigated by Einasto et al. (1994). For neighbourhood radii $\geq 32\, h^{-1}$ Mpc, almost all clusters join to form one huge percolating system. Thus it is clear that a meaningful neigh-

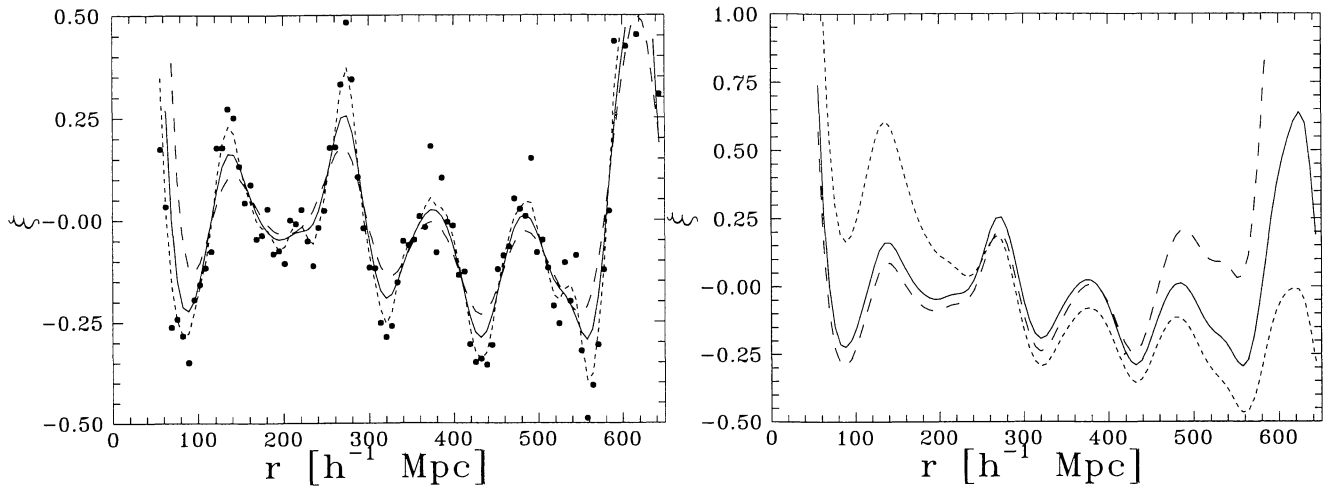

Figure 5. The influence of procedural artefacts on the correlation function. In the left-hand panel, for the sample with redshifts in rich superclusters, dots show the unsmoothed correlation function; short-dashed, solid and long-dashed lines show the correlation function smoothed with Gaussian dispersions 6.5, 13 and 20 h^{-1} Mpc, respectively. In the right-hand panel the influence of the selection function in the correlation function is given. The short-dashed line is for the selection function with parameters $s_0 = 0.14$, $d_0 = 1$, $d_1 = 0.50$; the solid line is for the selection function with $s_0 = 0.38$, $d_0 = 1$, $d_1 = 0.80$ (correct values); and the long-dashed line is for the selection function with $s_0 = 0.38$, $d_0 = 1$, $d_1 = 0.90$.

bourhood radius must be smaller than this value. If the radius is very small then we select as superclusters only the highest density peaks of the distribution of clusters, and the number of clusters in superclusters becomes too small for the determination of the correlation function. To determine the influence of this parameter, we compiled superclusters using a series of values of the neighbourhood radius: 12, 16 and 20 h^{-1} Mpc. For all cases the correlation function for clusters was calculated. The results indicate that with decreasing neighbourhood radius the amplitude of oscillations of the correlation function increases, since only very compact superclusters will be selected. However, the positions of the maxima are practically the same as for the adopted neighbourhood radius (24 h^{-1} Mpc). This test shows that the oscillating behaviour and parameters of oscillations are quite stable and do not depend on the choice of the neighbourhood radius.

4.4 Smoothing scale

To investigate the influence of the smoothing length on our results we calculated the correlation function for one sample with various values of the dispersion σ_s. Results are shown in Fig. 5. This calculation shows that there is no principal difference between results for different smoothing lengths. The main parameters of the correlation function (the period and positions of the maxima and minima) change only by a few per cent. The largest change is in the amplitude of oscillations, which decreases considerably with the increase of the smoothing length. To avoid the influence of the smoothing, we determined the amplitude from non-smoothed data. In all figures we have used a smoothing length of $\sigma_s = 13$–$15\,h^{-1}$ Mpc. This almost completely removes the Poisson noise, and is sufficient to investigate details of the correlation function above a scale of 30 h^{-1} Mpc.

4.5 Selection function

One frequently asked question concerns the influence of the selection function. If the feature investigated is of the same scale as the depth of the sample, then small errors in the selection function can seriously influence the results. To investigate the influence of the selection function in our case we calculated the correlation function of one sample for a number of different selection function parameters used in the calculation of comparison Poisson samples. Results are presented in Fig. 5. In all cases the same procedure was applied to calculate the selection function (discussed in Section 2 above). Only the parameters of the selection function were changed. As test sample, we chose clusters in rich superclusters (ACO.R.H8). In this case the number density of clusters decreases very rapidly with increasing distance from the Galactic pole (cf. Fig. 1). If we ignore this rapid decrease and adopt a standard value for the selection parameter (as for all clusters), $s_0 = 0.14$, then the overall mean slope of the correlation function changes. If we change the parameter that determines the decrease of the number density of the sample with distance and adopt too low a value for the number density on the far side of the sample ($d_1 = 0.9$ instead of the correct value $d_1 = 0.8$), then the whole correlation function on large scales increases. Both changes of selection function parameters have, however, little effect on the main parameters of the correlation function: none of the parameters quoted in Table 2 changes by more than a few per cent. Thus we can say that small errors of the selection function do not influence our main results. This insensitivity is due to the fact that the size of our sample is much larger than the scale of interest.

5 COMPARISON WITH MODELS

In this section we compare our empirical correlation function of clusters of galaxies with correlation functions calculated for several models. We use CDM models of structure evolution, and models with a double-power-law spectrum, as well as geometrical models with randomly and regularly located superclusters. Our main questions are: Can the observed correlation function of clusters of galaxies be reproduced by conventional models of structure evolution? If not, what changes in models are needed to reproduce the observed function?

5.1 Comparison with CDM models

We have calculated several N-body models of structure evolution. One model is based on the standard CDM scenario of structure formation. It has a structure parameter $\Gamma = \Omega h = 0.5$, with the Hubble parameter $h = 0.5$, and the density parameter $\Omega = 1$. The second model was calculated with a double-power-law perturbation spectrum, with spectral index $n = 1$ on large scales (wavenumber $k < k_0$), index $n = -1.5$ on small scales (wavenumber $k > k_0$), and the transition at wavelength $\lambda_0 = 2\pi/k_0 = 115\ h^{-1}$ Mpc. Models were calculated using a particle-mesh code with 128^3 particles and 256^3 cells in a cube of size $L = 700\ h^{-1}$ Mpc. Clusters of galaxies were searched with a method similar to the 'friends-of-friends' algorithm. The mass of clusters is determined from the number of particles in volumes of enhanced density. The lower limit of the mass of clusters was chosen so that the total number of clusters in the sample was in agreement with the mean spatial density of Abell–ACO clusters.

We calculated the correlation function of model clusters for the whole box using all clusters and also for double-conical subsamples of clusters in rich and poor superclusters. We applied a supercluster search algorithm identical to the one used for the search of real superclusters with neighbourhood radius $24\ h^{-1}$ Mpc. In each of our simulations we constructed three double-conical volumes (cone axes directed along the three axes) and searched clusters in these volumes. Clusters were divided into two populations – one in rich superclusters and the other in poor ones, with limiting richness $N_{\rm cl} = 8$ as in the real case. Correlation functions found for the CDM model are plotted in Fig. 6.

There are no regular oscillations in the correlation function in rich superclusters, either in the whole cubical sample or in the double-conical volumes. The correlation functions of simulated clusters in the double-conical volumes and located in rich superclusters have several peaks and valleys on large scales, but the location and amplitude of these peaks are random (for details see the next subsection). Model clusters in poor superclusters have a smooth correlation function close to zero at large scales.

This result is expected, as the power spectrum of CDM models is a smooth function of wavenumber, with a continuous change in the slope of the spectrum. For such spectra, oscillations of the correlation function are not expected, since oscillations occur only in the case when the spectrum has a peak and the slope near the peak changes suddenly (Frisch et al. 1995; Paper III).

This does not exclude the possibility that, in some realizations of a model with a CDM-type perturbation spectrum, peaks and valleys in the correlation function of clusters in rich superclusters are located more regularly. This occurs when the perturbation spectrum accidently has an extra peak near its maximum. In the next subsection we study more closely the possibility of how frequently such a peak can occur.

5.2 Comparison with random supercluster samples

To investigate the possible generation of regular oscillations in the correlation function for double-conical volumes of clusters in rich superclusters, we must generate a large number of realizations of models. The distribution of clusters in models is determined essentially by medium-scale perturbations which are still in the linear stage of evolution. Thus it is not necessary to use conventional N-body calculations of structure evolution. Borgani et al. (1995) have used the Zeldovich approximation for a similar task. In this paper we shall apply an even simpler procedure to investigate the regularity of the large-scale distribution of clusters.

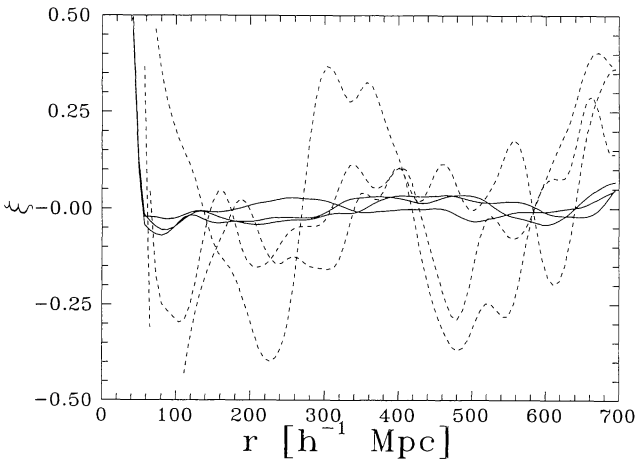

Figure 6. The correlation functions of clusters for CDM models. Solid lines are for clusters in double-conical subsamples located in poor superclusters (with fewer than eight members), and dashed lines are for clusters in double-conical volumes in rich superclusters (with at least eight members).

In the present problem it is not essential to use exactly the CDM spectrum. What is important is to apply a broad-band spectrum with a smooth transition between regions at large and short wavelengths. As demonstrated in Paper III, the power spectrum of the random supercluster model is rather similar to the power spectrum of CDM models, in particular in the medium-wavelength region of interest for the present study. Correlation functions of these models are also very similar. We make use of this similarity and generate a large number of realizations for the random supercluster model to see how frequently such a model can reproduce properties of the real correlation function.

In this model (for details, see Paper III) superclusters are located randomly in space. They contain clusters of galaxies in numbers that are in agreement with the observed multiplicity function of superclusters. To imitate the observations, we choose a double-conical sub-volume from the whole cubical sample and select clusters that belong to rich superclusters with at least eight member clusters. The full side length of the cube is taken to be $L = 700\ h^{-1}$ Mpc. The number of superclusters in models is taken to be approximately equal to 650; in this case the number of clusters in rich superclusters of double-conical subsamples is about 300 as in the observed cluster sample in rich superclusters. Our calculations show that the correlation function of this model also has maxima and minima, but they are located randomly, similar to the cluster correlation function of CDM models. We can characterize oscillations and their regularity by the following parameters: the mean period of oscillations, its rms scatter, the mean amplitude of oscillations, and its rms scatter.

Results of our calculations for 1000 realizations of the random supercluster model are shown in Fig. 7, separately for the amplitude versus period and for the scatter of the amplitude versus the scatter of the period. If a point lies outside the 1 per cent contour, it has a probability of occurrence of <1 per cent. We see that for both variable parameter pairs the observational point lies just outside the 1 per cent contour. In other words, the probability that our observed sample is taken from the same model is approximately 1 per cent for both variable pairs.

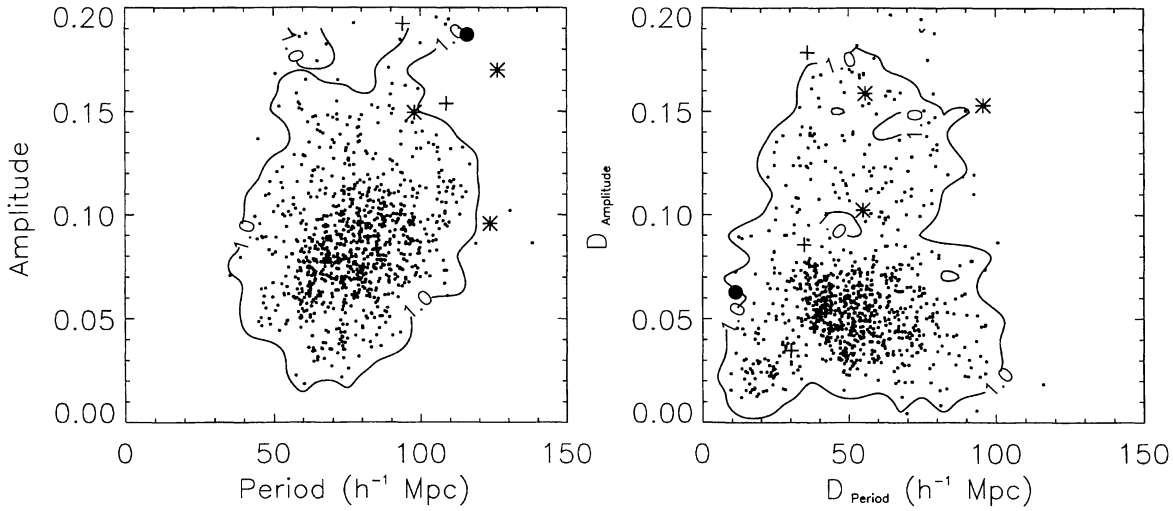

Figure 7. Parameters of oscillations of the correlation function: period, amplitude (left-hand panel), and their scatters, $D_{\rm Period}$, $D_{\rm Amplitude}$ (right-hand panel). The large filled circle shows the observed values for clusters in rich superclusters (sample ACO.R.H8); dots are respective values for 1000 realizations of the random supercluster model, crosses are for the standard CDM model, and stars are for a low-density CDM model with cosmological constant (see Paper III for details). Contours indicate the probability level for random superclusters outside which 1 per cent of periods and amplitudes are found. To calculate parameters of oscillations for this figure we used smoothed correlation functions. In this case the amplitude of oscillations from observations is $A = 0.186$ (the value given in Table 2 corresponds to the amplitude of the unsmoothed correlation function).

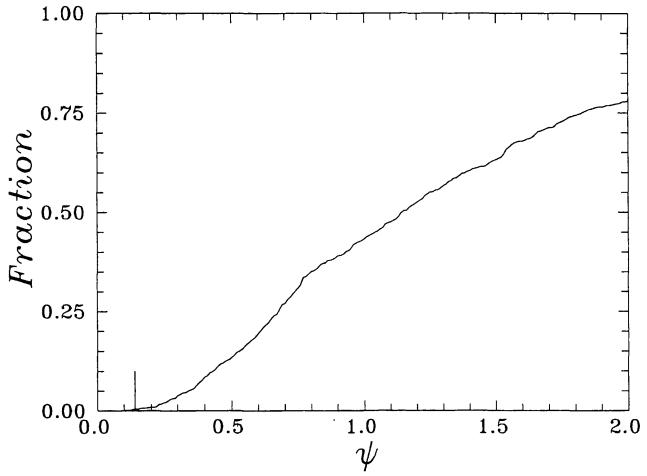

Figure 8. The integrated frequency distribution of the correlation function variance parameter ψ. The observed value of ψ is noted by a vertical bar.

We applied a further test using the fine details of the correlation function. As noted above, the position of the first secondary maximum of the correlation function, as well as mean differences between the second and first, and between the third and second maxima, is in certain fixed relations with the period of oscillation. We can define a correlation function variance parameter as follows:

$$\psi^2 = (f_0 - f_{00})^2 + (f_1 - f_{10})^2 + (f_2 - f_{20})^2, \quad (6)$$

where f_0, f_1 and f_2 are values of parameters defined by equations (12)–(14) of Paper III and found for the test model; f_{00}, f_{10} and f_{20} are respective values calculated for the geometric model with regular structure. As demonstrated in Paper III, these parameters are rather stable and depend only little on models with different details of the structure. Essential is the presence of a regular network of superclusters and voids. Thus we have calculated the correlation function variance parameter ψ for all our 1000 test models (see Fig. 8).

This calculation shows that the mean value of the parameter is $\psi = 1.4$. The distribution is very asymmetric with a long tail towards large ψ-values. The lowest value for these 1000 realizations is 0.1. The observed value is $\psi \approx 0.14$. We see that the probability that the observed case is taken randomly from the family of random supercluster models is also about 1 per cent. All our variables used in these tests are independent of each other, and thus the probability of obtaining all five parameters fitted once by the random supercluster model simultaneously is much smaller than 1 per cent.

Even if using the random supercluster model were a fast but not ideal procedure for calculating these probabilities, the main result would be hardly changed by more ingenious simulations: the probability is very small. Thus we conclude that within standard cosmological models it is difficult to generate the observed correlation function.

6 POWER SPECTRUM

Which perturbation spectrum can produce the observed correlation function of clusters in rich superclusters? Analytic calculations made in Paper III show that the correlation function has an oscillatory behaviour only if the power spectrum has a peak at the corresponding wavenumber. In this paper it was also demonstrated that the sharpness and height of the peak in the spectrum determine the character of oscillations of the correlation function.

Here we estimate the possible shape of the spectrum on scales of interest using comparison with models with known spectra. We shall compare the spectra and correlation functions of three models: the standard CDM model, the double-power-law model, and a mixed geometrical model consisting of two populations, one with superclusters located randomly along regularly spaced rods and the other with irregularly spaced superclusters (see Paper III for details). Power spectra of these three models are shown in Fig. 9.

We see that the double-power-law model and the mixed model have rather similar spectra near the maximum. Both models also have similar correlation functions with weak oscillations (see fig. 4 of Paper III). The oscillations are more regular in the geometrical

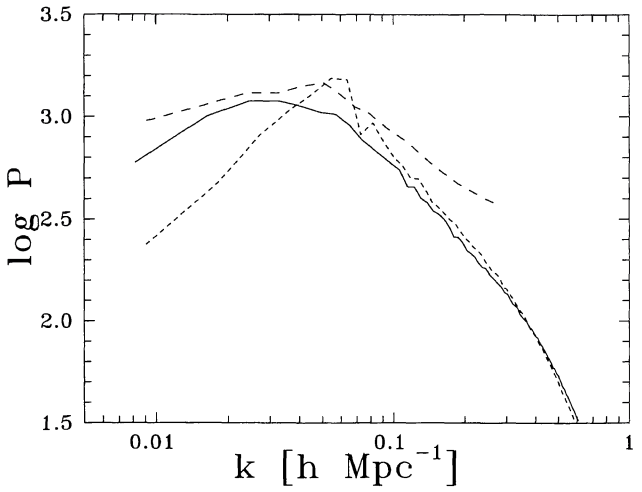

Figure 9. Power spectra for the CDM model, the double-power-law model, and the mixed geometrical model, plotted with solid, short-dashed, and long-dashed lines, respectively.

model, as expected. However, the differences between models are not large. The maximal deviation of the spectrum near the maximum from the corresponding CDM-type spectrum is ~0.2 dex, i.e. about a factor of 1.25 in amplitude.

These models show that already a modest deviation from the standard CDM spectrum produces an oscillating correlation function for clusters in rich superclusters.

The actual power spectrum of our cluster sample has a peak of even higher amplitude (see E97).

7 CONCLUSIONS

We have determined the correlation function for clusters of galaxies separately for all clusters and for clusters located in rich and in poor superclusters. The correlation function of clusters in rich superclusters that form the skeleton of the supercluster–void network has an oscillatory behaviour with a period of $115 \pm 15\,h^{-1}$ Mpc. Within an interval of $\sim 650\ h^{-1}$ Mpc over which observational data are available, five secondary maxima and minima of the correlation function are seen. The amplitude of oscillations is larger for clusters located in very rich superclusters.

The scale of the supercluster–void network found here on the basis of the cluster correlation function is rather close to the scale found using other methods, such as void diameter analysis, pencil-beam studies, or absorbers in the line of sight to QSOs (Quashnock et al. 1996), although the latter apply to higher redshifts.

The reality of oscillations of the cluster correlation function is supported by the following arguments. (1) The error corridor of the correlation function determined for clusters in rich superclusters is much smaller than the amplitude of oscillations. (2) Oscillations are seen in cluster samples located in both Galactic hemispheres. (3) Similar oscillations with lower amplitude are observed in the Las Campanas Redshift Survey of galaxies by Tucker et al. (1995, 1997). (4) In all samples the shape of the oscillating correlation function follows almost exactly the expected shape for a quasi-regular network of superclusters and voids. (5) The double-conical shape of the volume sampled by clusters cannot influence the results. (6) Parameters of the oscillations practically do not depend on the smoothing length of the correlation function, or on the neighbourhood radius used in supercluster definition, or on errors of the selection function used to calculate the correlation function.

The correlation length of clusters of galaxies depends on the cluster population: for clusters in poor superclusters it is about $17\,h^{-1}$ Mpc; for clusters in rich superclusters it is about 45 h^{-1} Mpc.

We have compared the observed correlation function with correlation functions calculated for clusters in CDM models and for models with randomly distributed superclusters. These models have a broad-band power spectrum with a smooth transition between the positive spectral index at long wavelengths and a negative index at small wavelengths. In these models the correlation function of clusters in rich superclusters located in double-conical volumes also has peaks and valleys, but these peaks and valleys are distributed randomly and have random amplitudes. The probability that a model with a broad-band power spectrum has parameters of oscillations of the correlation function similar to observed parameters is very low ($\ll$1 per cent).

Analytical calculations show that oscillations of the correlation function appear only in the case that the power spectrum has a peak at the wavelength equal to the period of oscillations. We have compared spectra and correlation functions of models with various heights of the peak in the spectrum. These calculations show that it is possible to generate an oscillating correlation function for clusters in rich superclusters if the height of the peak is of the order of a factor of at least 1.25 in amplitude over the conventional smooth spectrum.

The fact that the amplitude of oscillations near the last maximum is still rather large suggests that the coherence of positions of high-density regions extends over very large separations (at least 10 per cent of the diameter of the observable Universe).

ACKNOWLEDGMENTS

This work was supported by Estonian Science Foundation grant 182 and International Science Foundation grant LLF100. We thank Bernard Jones, Jerry Ostriker and Jim Peebles for discussions. JE and AAS were supported by the Deutsche Forschungsgemeinschaft in Potsdam; AAS was supported by the Russian Research Project 'Cosmomicrophysics'.

REFERENCES

Abell G., 1958, ApJS, 3, 211
Abell G., Corwin H., Olowin R., 1989, ApJS, 70, 1 (ACO)
Andernach H., Tago E., Stengler-Larrea E., 1995, Astrophys. Lett. Commun. 31, 27
Bahcall N. A., 1991, ApJ, 376, 43
Bahcall N. A., Soneira R. M., 1983, ApJ, 270, 20
Bond J. R., Efstathiou G., 1984, ApJ, 285, L45
Borgani A., Plionis M., Coles P., Moscardini L., 1995, MNRAS, 277, 1191
Broadhurst T. J., Ellis R. S., Koo D. C., Szalay A. S., 1990., Nat, 343, 726
Dekel A., Blumenthal G. R., Primack J. R., Olivier S., 1989, ApJ, 338, L5
Dekel A., Blumenthal G. R., Primack J. R., Stanhill D., 1992, MNRAS, 257, 715
Doroshkevich A. G., Tucker D. L., Oemler A., Kirshner R. P., Lin H., Shectman S. A., Landy S. D., Fong R., 1996, MNRAS, 283, 1281
Einasto J., Gramann M., 1993, ApJ, 407, 443
Einasto J., Gramann M., Saar E., Tago E. 1993, MNRAS, 260, 705
Einasto J. et al., 1997a, Nat, 385, 139 (E97)
Einasto J. et al., 1997b, MNRAS, 289, 813 (Paper III, this issue)

Einasto M., Einasto J., Tago E., Dalton G., Andernach H., 1994, MNRAS, 269, 301
Einasto M., Tago E., Jaaniste J., Einasto J., Andernach H., 1997c, 1997c, A&AS, 123, 119 (Paper I, astro-ph/9610088)
Fetisova T. S., Kuznetsov D. Y., Lipovetskij V. A., Starobinsky A. A., Olowin R. P., 1993, Pis'ma Astron. Zh., 19, 508 (English Translation: Astron. Lett., 19, 198)
Frisch P., Einasto J., Einasto M., Freudling W., Fricke K. J., Gramann M., Saar V., Toomet O., 1995, A&A, 296, 611
Kaiser N., Peacock J. A., 1991, ApJ, 379, 482
Kopylov A. I., Kuznetsov D. Y., Fetisova T. S., Shvarzman V. F., 1984, Astron Tsirk., 1347, 1
Kopylov A. I., Kuznetsov D. Y., Fetisova T. S. & Shvarzman V. F., 1988, in Audouze J., Pelletan M.-C., Szalay A. eds, Large-Scale Structure of the Universe. Kluwer, Dordrecht, p. 129
Landy S. D., Shectman S. A., Lin H., Kirshner R. P., Oemler A. A., Tucker D., 1996, ApJ, 456, L1
Mo H. J., Xia X. Y., Deng Z. G., Börner G., Fang L. Z., 1992a, A&A, 256, L23
Mo H. J., Deng Z. G., Xia X. Y., Schiller P., Börner G. 1992b, A&A, 257, 1
Mo H. J., Jing Y. P., Börner G., 1992c, ApJ, 392, 452
Peacock J. A., West M. J., 1992, MNRAS, 259, 494
Quashnock J. M., Vanden Berk D.E., York D.G., 1996, ApJ, 472, L69
Saar V., Tago E., Einasto J., Einasto M., Andernach H., 1995, astro-ph/9505053
Sutherland W., 1988, MNRAS, 234, 159
Tucker D. L. et al., 1995, BAAS, 27, 1365
Tucker D. L. et al., 1997, MNRAS, 285, L5
Zwicky F., Wild P., Herzog E., Karpowicz M., Kowal C. T., 1961–68, Catalogue of Galaxies and of Clusters of Galaxies, Vols I – VI. California Inst. Tech., Pasadena

This paper has been typeset from a TEX/LATEX file prepared by the author.